

# Carrier-Phase DNS of Biomass Particle Ignition and Volatile Burning in a Turbulent Mixing Layer

Martin Rieth<sup>\*a</sup>, Miriam Rabaçal<sup>b</sup>, Andreas M. Kempf<sup>a</sup>, Andreas Kronenburg<sup>c</sup>, Oliver T. Stein<sup>c</sup>

<sup>a</sup> Fluid Dynamics, Institute for Combustion and Gas Dynamics, University of Duisburg-Essen, Germany

<sup>b</sup> Aerothermochemistry and Combustion Systems Laboratory, ETH Zürich, Switzerland

<sup>c</sup> Institut für Technische Verbrennung, Universität Stuttgart, Germany

[martin.rieth@uni-due.de](mailto:martin.rieth@uni-due.de)

Direct numerical simulations (DNS) of a three-dimensional turbulent mixing layer are performed to study the volatile ignition and combustion behavior of biomass under conditions relevant for industrial applications. The DNS is designed such that it resolves the flame and all turbulent scales, but reverts to a point-particle description to avoid the resolution of individual particle boundary layers. The biomass particles are seeded in an air stream and mix with hot products from a second stream. The particles are heated up as they mix with the hot gases in the developing turbulent mixing layer. This is followed by devolatilization and volatile combustion. The volatile gas composition is modeled based on the composition and properties of the biomass particles. The gas phase is described by a reduced mechanism with 59 species and 462 reactions derived from the CRECK primary reference fuel and biomass mechanisms. The simulations are performed with the in-house LES/DNS code PsiPhi, coupled to Cantera to evaluate gas phase kinetics. The data is analyzed in terms of instantaneous contour plots of relevant quantities as well as spatially averaged statistics. The results are compared to a case of coal burning in the identical mixing layer setup such that differences and similarities between the ignition and burning behavior of biomass and coal can be analyzed. Both cases feature only small amounts of char conversion, hence the focus lies on volatile combustion. While zero-dimensional reactor calculations predict an earlier ignition of the volatiles from biomass for some conditions and biomass particles heat up faster, it is found that biomass ignites later than coal in the mixing layer. This is associated with the higher stoichiometric mixture fraction and lower heat release of the volatile-air mixture from biomass.

## 1. Introduction

Pulverized coal combustion (PCC) is presently one of the major technologies for the production of electricity. However, its CO<sub>2</sub> footprint is worse than that of other fossil fuel technologies (e.g., combustion of natural gas). A way to mitigate CO<sub>2</sub> release is to (partially or fully) replace coal by biomass. The use of computational fluid dynamics (CFD) can, along with detailed experiments, provide understanding of the physics and chemistry of (turbulent) combustion of coal and biomass, and aid combustor design to reduce emissions. While large eddy simulations (LES) are increasingly used to study turbulent combustion up to the industrial scale, smaller turbulent multiphase reaction systems can be addressed by means of direct numerical simulations (DNS), which also allows for the development of subgrid models for LES. In a previous study, we have conducted DNS of a coal particle laden mixing layer with a relatively detailed homogenous chemical mechanism containing 52 species, to study volatile ignition and combustion and to provide a database for solid-to-gas multiphase combustion modeling (Rieth et al. 2018). Some DNS studies of biomass pyrolysis and combustion have emerged recently, however, the description of the devolatilization and combustion chemistry required considerable simplifications (Russo et al. 2014; Awasthi et al. 2016). Specifically, devolatilization was considered to be governed by a characteristic temperature (Russo et al. 2014), or gas phase chemistry was described by a reduced 6 species scheme (Awasthi et al. 2016). In recent years, there have been substantial improvements on the phenomenological understanding of biomass devolatilization, concerning detailed decomposition kinetics, primary product speciation, secondary gas-phase decomposition and gas phase

oxidation. Ranzi and co-authors (Ranzi et al. 2005; Ranzi et al. 2008) proposed a biomass pyrolysis mechanism with 46 species, that includes sub-mechanisms to describe the pyrolysis of the three reference components of biomass: cellulose, hemicellulose, and lignin. No interaction of the components is assumed, which is commonly supported in the literature (Di Blasi 2008). In this way, the pyrolysis primary products of a certain biomass can be described as the weighted sum of the yields of the individual components present in the raw biomass. This allows for a universal description of the biomass composition regardless of its origin (Rabaçal et al. 2018). The primary pyrolysis products will undergo successive decomposition and combustion reactions in the surrounding gas phase. A detailed homogeneous kinetic mechanism of the secondary gas-phase pyrolysis, partial oxidation and combustion of species released during biomass pyrolysis, was developed by Ranzi and co-authors (Ranzi et al. 2008), with 137 species and 4533 reactions, including the thermodynamic properties of the involved species, as well as a comprehensive set of primary propagation reactions. The application of these detailed chemical models directly to DNS is prohibitive, but reduced mechanisms can be used, as demonstrated in a previous study for coal (Rieth et al. 2018).

The main objective of this work is to study the volatile ignition and combustion behavior of pine under conditions relevant for industrial applications using DNS, and to compare the behavior of pine with that of coal (Rieth et al. 2018). While a similar subject has been considerably studied using laboratory-scale experimental techniques at both laminar and turbulent conditions (Rabaçal et al. 2018), DNS studies with relatively detailed volatile compositions and corresponding homogeneous chemistry are scarce. In this work, the primary volatile composition is first obtained using the detailed biomass pyrolysis mechanism by Ranzi et al. (2008). The biomass volatile composition is then simplified and coupled to a reduced 59 species mechanism for homogeneous chemistry, which is validated against the detailed homogeneous mechanisms by Ranzi and co-workers (Ranzi et al. 2008). Finally, the reduced mechanism is directly integrated in the DNS and the DNS results for biomass combustion are compared to the previous coal DNS data for the same turbulent mixing layer configuration. To focus on volatile ignition and combustion as an initial step, the devolatilization kinetics in the DNS are unchanged compared to the coal case.

## 2. Numerical Approach and Computational Configuration

### 2.1 Raw biomass properties

The composition of pine in terms of ultimate and proximate analysis was retrieved from the review by Rabaçal et al. (2018). The reference composition of the biomass is obtained on the basis of the ultimate analysis using a method developed by Cuoci et al. (2007). Because of the complexity of the lignin structure, three species identified as LIG-C, LIG-O, and LIG-H are used in the devolatilization mechanism (Ranzi et al. 2008), which are rich in carbon, oxygen, and hydrogen, respectively. Three reference biomass fuels (S1, S2, and S3) with specific oxygen/carbon and hydrogen/carbon ratios are defined as linear combinations of the five components (cellulose, hemicellulose, and the three lignin species), setting up a triangle. Any biomass contained in the range of hydrogen and carbon enclosed by the triangle vertices can be described as a linear combination of the reference biomass fuels. Using this method, the obtained biomass composition, in wt% daf, is 53.27 of cellulose, 25.51 of hemicellulose, 1.704 of LIG-C, 9.051 of LIG-H and approximately 0.0 of LIG-O. The estimated content of lignin is rather low (~10 wt% daf), as compared to typical values observed experimentally, but the composition is consistent with the fact that the method typically yields a negligible amount of the oxygen-rich lignin compound (Ferreiro et al. 2017). Considering that the value is within the expected order of magnitude, and within the scope of the present study, the lignin content and biomass composition are considered reasonable.

### 2.2 Pyrolysis characteristics and primary volatile composition

The pyrolysis mechanism from Ranzi et al. (2008), with 26 species and 47 reactions, was used to calculate the pyrolysis rate and final products of primary pyrolysis. The species conservation was solved using the stiff differential equations solver from Shampine et al. (1999), for which the reaction rates were calculated with the Kinetics library from Cantera (Goodwin et al. 2017). A heating rate of  $10^5$  K/s was used, as observed in our previous DNS study with coal (Rieth et al. 2018). This value was used for the calculations in this work. Figure 1 shows the predicted devolatilization rate (a), and the final volatile composition (b).

Similar to our previous DNS study (Rieth et al. 2018), the volatile composition is considered constant throughout the devolatilization process and corresponds to the final total volatile yield. This is generally the case for cellulose and hemicellulose (Ferreiro et al. 2017), and since both present similar devolatilization profiles (see Figure 1(a)), it is fair to assume that the combined volatile mixture from both components is equal to the sum of the individual component profiles. This is not strictly true for lignin, which is also related to its typical bimodal devolatilization curve (Ferreiro et al. 2017) as shown in Figure 1(a). However, considering that

the lignin content is only ~10 %, we neglect the variation of the volatile composition with devolatilization progress. As can be observed in Figure 1(b), large amounts of hydroxy-acetaldehyde ( $C_2H_4O_2$ ) are present in the volatile gas, which is one of the main primary volatile products of cellulose (Piskorz et al. 1986). Given that cellulose is the main component of pine, this result is not surprising. Further, relatively large amounts of  $C_6H_6O_3$ ,  $CO_2$ ,  $CO$  and  $H_2O$  are formed during pyrolysis.

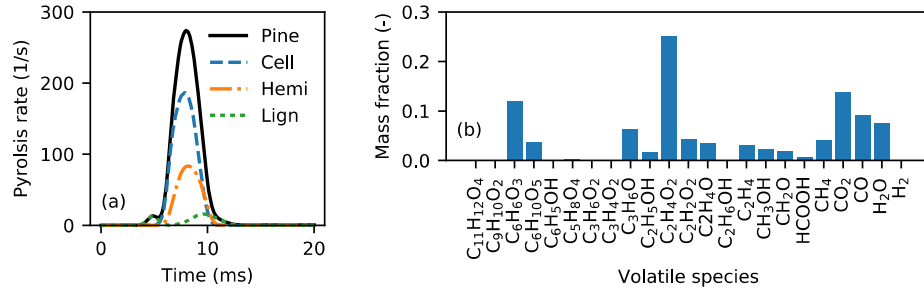


Figure 1. Pyrolysis characteristics of pine, heating rate 105 K/s: (a) devolatilization rate, (b) volatile species.

### 2.3 DNS problem configuration

The gas phase is described by the variable-density equations of mass, momentum and enthalpy. These governing equations include additional source terms for the interaction with the solid particle phase. The details of the gas phase description are given in our earlier work (Rieth et al., 2018). Coal and biomass particles are described in a Lagrangian framework with the solution of the equations for particle position, velocity, acceleration, mass and temperature. Devolatilization is modelled by a competing rates model with the same rates as for coal reported earlier (Rieth et al., 2018). Here, to solely focus on the differences between biomass in coal combustion with respect to the gas phase kinetics, we retain the same devolatilization sub-model for the DNS as for our earlier coal case. Along the same lines, the other models regarding thermal and radiative properties, heat transfer and Stefan flow are treated in the same way as in the coal case. The main difference between the coal and biomass particles from the modelling perspective is a reduction of the density by a factor of 2 while keeping the mass of a single particle constant and the change of volatile gas composition described previously. The DNS setup follows the earlier work closely. The top stream consists of air at 600 K with solid fuel particles. The bottom stream consists of a lean volatile product mixture. Due to the modified stoichiometry (stoich. mixture fraction of 0.169 for biomass, compared to 0.095 for the coal case), the initial volatile mixture fraction in the bottom stream was modified to 0.0797 (0.043 for the coal case), to keep the bottom stream temperature the same as in the coal case (1693 K).

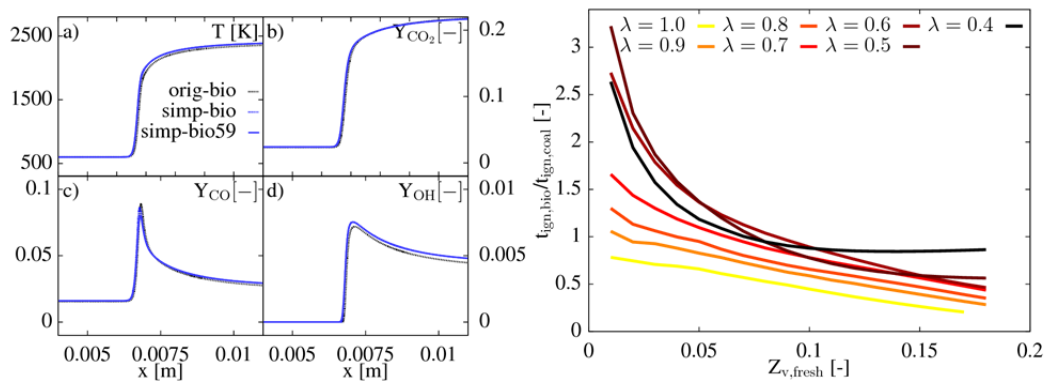


Figure 2. Left (a): Stoichiometric premixed flame with original volatile composition calculated with the full biomass mechanism (orig-bio), the simplified composition calculated with the full biomass mechanism (simp-bio) and the simplified composition calculated with the reduced 59 species mechanism (simp-bio59). Right (b): ratio of homogeneous ignition delay times of biomass and coal volatiles as a function of fresh volatile mixture fraction ( $Z_{v,fresh}$ , excluding the initial hot products) and different oxidizer compositions ( $\lambda = 1$ , pure hot products from lower stream,  $\lambda = 0$  pure air at 600 K from upper stream).

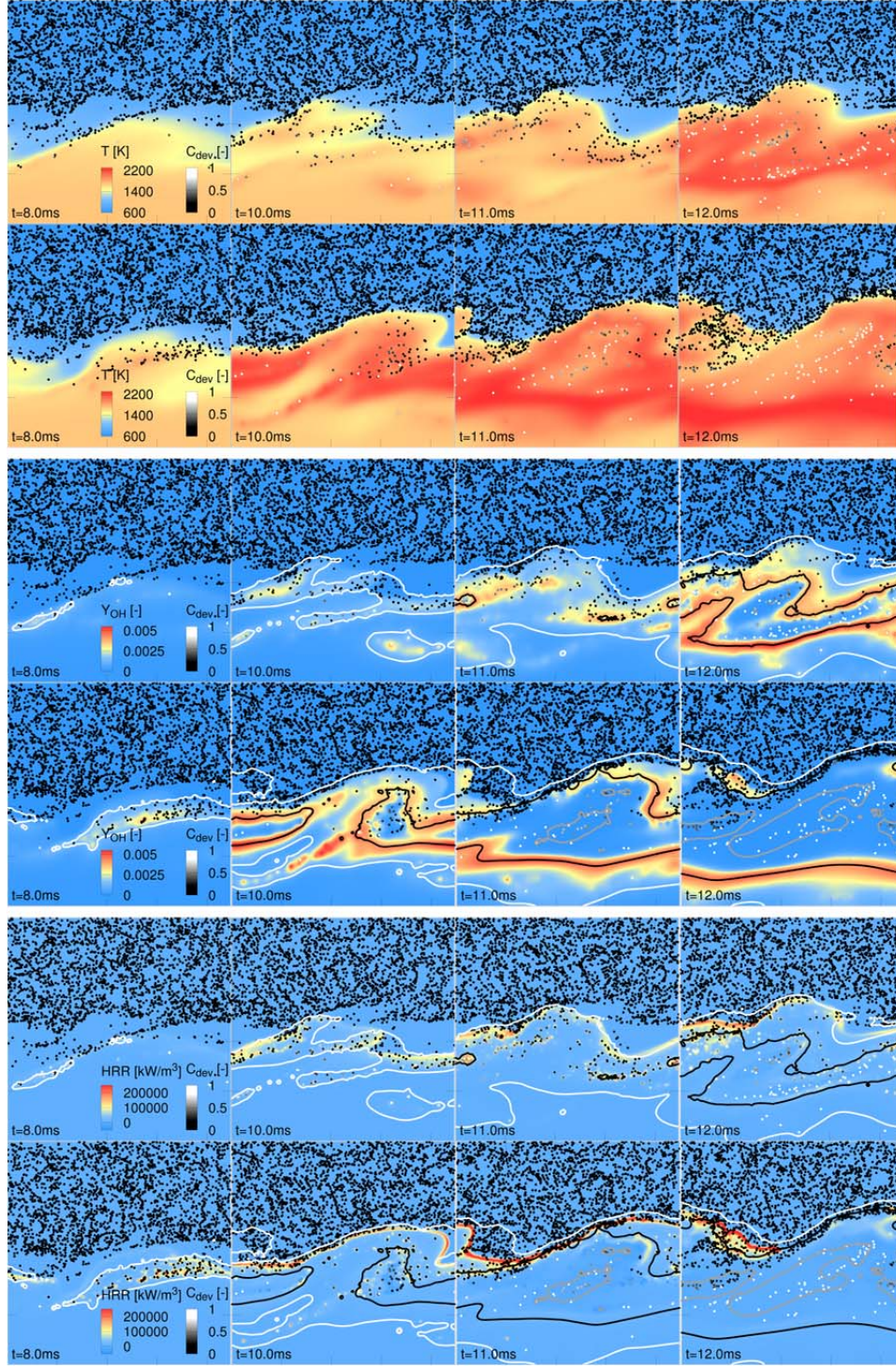


Figure 3. Temperature, OH mass fraction and heat release rate at selected times for biomass (top) and coal (bottom) cases. The iso-lines correspond to volatile mixture fractions  $Z$  of  $Z_{st}/2$  (white),  $Z_{st}$  (black) and  $2Z_{st}$  (grey), where  $Z_{st}$  is calculated with pure air as oxidizer ( $Z_{st}=0.169$  for biomass and  $Z_{st}=0.095$  for coal).

## 2.4 Gas-phase reaction model

The gas-phase reaction mechanism builds up on our previous study (Rieth et al. 2018) where we used a reduced 52 species kinetic model derived from the CRECK primary reference fuel mechanism (Ranzi et al. 2005, Stagni et al. 2016). However, some of the species from the detailed biomass volatile composition outlined in the previous section are not included in the reduced homogeneous mechanism. As a first step towards DNS of biomass combustion, we simplified the biomass volatile composition slightly by excluding

species with low mass fractions. In addition, we added the missing species and initial decomposition reactions (without modification of reactions and reaction rates) to the reduced mechanism originally designed for coal volatile ignition. A comparison of ignition delay times from homogeneous reactors and 1D premixed flame propagation calculations with the full biomass volatile mechanism (Ranzi et al. 2008) yields satisfactory results. The final mechanism consists of 59 species and 462 reactions. Compared to the coal case, the following species have been added to the mechanism:  $C_2H_4O_2$ ,  $C_2H_2O_2$ ,  $C_2H_4O$ ,  $C_3H_6O$ ,  $C_6H_{10}O_5$ ,  $C_4H_6O_2$ ,  $C_5H_8O_4$ . An exemplary comparison of the flame propagation case at stoichiometric conditions is presented in Figure 2(a). It shows the conversion of the original volatile composition calculated with the full biomass mechanism, the simplified composition calculated with the full biomass mechanism and the simplified composition calculated with the reduced 59 species mechanism. The flame speed between the cases varies by less than 2 %. Figure 2(b) illustrates the differences in ignition delay times between volatile air mixtures for biomass and coal. For values of the fresh volatile mixture fraction of less than 0.1 volatile ignition is faster for biomass than for coal if the oxidizer consists of hot products from the lower stream ( $\lambda \rightarrow 1$ ), but slower, if the oxidizer tends towards pure air ( $\lambda \rightarrow 0$ ). For values of the fresh volatile mixture fraction  $Z_{v, fresh} > 0.1$  biomass volatile ignition is always faster than for coal, irrespective of the oxidizer composition. This implies that isolated biomass particles travelling into the lower stream (hot lean products) will ignite faster than their coal counterparts. However, smaller biomass particle clouds or isolated particles in intermediate, colder mixtures (temperature between 600 and 1693K) will ignite more slowly than their coal counterparts.

### 3. Results

Figure 3 presents an overview of the evolution of temperature, OH mass fraction and heat release rate for biomass and coal at selected times around ignition for both cases. As can be observed, ignition occurs earlier in the coal case. Even though 0D reactor calculations showed biomass volatiles to produce shorter ignition delay times in hotter mixtures (containing large amounts of fluid from the lower stream) than the coal volatiles, the ignition of biomass in the 3D mixing layer is delayed compared to the coal case. It should be noted that due to the larger diameter and lower density of biomass particles, heating and devolatilization occur faster for biomass compared to coal particles. However, this effect cannot compensate the delayed homogeneous ignition. The slower ignition can be related to the difference in stoichiometry between coal and biomass volatile gases. The biomass volatile gas has a stoichiometric mixture fraction of 0.169 while that of coal is 0.095. This means that a larger amount of volatiles is required for the biomass case to reach ignition conditions. A larger amount of volatiles, however, leads to lower mixture temperatures, since fresh volatiles are colder than the hot gas in the lower stream. This is reflected in the fields for OH mass fraction and heat release rate. Conditions above  $Z_{st}/2$  are reached earlier in the coal case, resulting in earlier ignition, OH production and heat release. At early times ( $t=8$  ms), heat release can mostly be observed around individual particles or particle groups in the coal case. This behavior is not observed in the contour plots of the biomass case. The contour plots of the biomass case rather show group combustion behavior at later times. Similar to the coal case, a formation of lean flame fronts that can be associated with the premixed combustion mode (not shown here for brevity) can be observed in the biomass case. However, peak heat release rates remain lower than in the coal case due to a lower heating value of the biomass volatile gas (heat released at stoichiometric equilibrium conditions: 15.7 MJ/kg for biomass, 28.0 MJ/kg for coal), which affects heating and devolatilization.

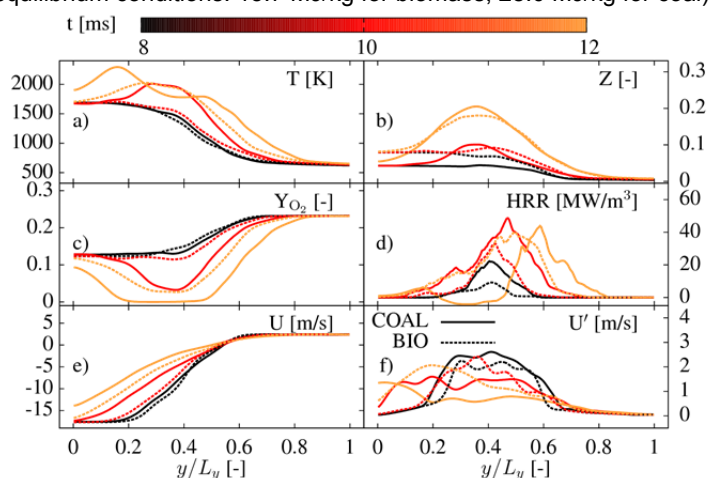


Figure 4. Plane-averaged temperature, volatile mixture fraction,  $O_2$  mass fraction, heat release rate, streamwise velocity and streamwise velocity fluctuation for coal (continuous lines) and biomass (dotted lines).

Figure 4 presents spatially averaged profiles of temperature, volatile mixture fraction, O<sub>2</sub> mass fraction, heat release rate, streamwise velocity and velocity fluctuations. Figure 4 confirms the observations from the contour plots presented in Figure 3. The coal case shows a more rapid temperature increase, which is tightly coupled to the increase in mixture fraction. The earlier ignition is reflected in the faster decay of oxygen in the middle of the mixing layer. At 12 ms, the biomass case coincidentally shows a heat release rate profile similar to that of coal at 10 ms, indicating slower conversion of biomass than coal (by approximately 2 ms). At that time, parts of the computational domain for the coal case show very rich mixtures and even negative heat release rates, as CO<sub>2</sub> is slowly converted to CO by an endothermic reaction (Rieth et al. 2018).

#### 4. Conclusions

This work presents a first-of-its-kind carrier-phase DNS of biomass combustion in a turbulent mixing layer using a detailed, yet tractable, volatile composition and homogeneous chemistry. The results for this biomass case are compared to an earlier case of coal combustion in the same mixing layer configuration, where the pyrolysis kinetics for coal and biomass are kept identical to allow for a direct comparison. While 0D reactor calculations indicate an earlier ignition of the volatiles from biomass for some conditions and biomass particles heat up faster, the biomass ignites later than coal in the 3D-DNS, which is associated with the higher stoichiometric mixture fraction and lower heat release of the volatile-air mixture for biomass. Future work is required to check the generality of this result and to incorporate more detailed models for biomass thermal conversion, i.e., devolatilization modeling, drying, thermal properties, etc.

#### Acknowledgments

The authors are grateful for financial support by a Postdoctoral Fellowship from ETH Zurich (M. Rabaçal) and DFG Germany, grant numbers KR 3684/8-1, KE 1751/3-1, HA 4367/3-1. We acknowledge computing time at the Center for Computational Sciences and Simulation of the University of Duisburg-Essen (CCSS/ZIM) on the supercomputer magnitude, DFG grants INST 20876/209-1 FUGG, INST 20876/243-1 FUGG.

#### References

- Awasthi, A., Kuerten, J. G. M., Geurts, B.J., 2016, Direct numerical simulation of biomass pyrolysis and combustion with gas phase reactions. *J. Phys.: Conf. Ser.* 2016, 745, 032119.
- Cuoci, A., Faravelli, T., Frassoldati, A., Granata, S., Migliavacca, G., Pierucci, S., Ranzi, E., Sommariva, S. A., 2007, General Mathematical Model of Biomass Devolatilization. Note 2. Detailed Kinetics of Volatile Species, 30th Meeting of the Italian Section of the Combustion Institute, Ischia, Naples, Italy, June 20–22.
- Di Blasi, C., 2008, Modeling chemical and physical processes of wood and biomass pyrolysis, *Progress in Energy and Combustion Science*, 34, 47–90.
- Ferreiro, A.I., Guidicianni, P., Grottola, C.M., Rabaçal, M., Costa, M., Ragucci, R., 2017, Unresolved issues on the kinetic modeling of pyrolysis of woody and non-woody biomass fuels, *Energy & Fuels*, 31, 4035–4044.
- Goodwin, D.G., Moffat, H.K., Speth, R.L., 2017, Cantera: An Object-Oriented Software Toolkit for Chemical Kinetics, Thermodynamics, and Transport Processes.
- Rabaçal, M., Pereira, S., Costa, M., 2018, Review of Pulverized Combustion of Non-Woody Residues, *Energy & Fuels*, 32, 4069–4095.
- Piskorz, J., Radlein, D., Scott, D.S., 1986, On the mechanism of the rapid pyrolysis of cellulose, *Journal of Analytical and Applied Pyrolysis*, 9(2), 121–137.
- Ranzi, E., Cuoci, A., Faravelli, T., Frassoldati, A., Migliavacca, G., Pierucci, S., Sommariva, S., 2008, Chemical kinetics of biomass pyrolysis, *Energy & Fuels*, 22, 4292–4300.
- Ranzi, E., Frassoldati, A., Granata, S., Faravelli, T., 2005, Wide-range kinetic modeling study of the pyrolysis, partial oxidation, and combustion of heavy n-alkanes, *Indus. & Eng. Chem. Res.* 44(14), 5170–5183.
- Rieth, M., Kempf, A.M., Kronenburg, A., Stein, O.T., 2018, Carrier-phase DNS of pulverized coal particle ignition and volatile burning in a turbulent mixing layer, *Fuel*, 212, 364–374.
- Russo, E., Kuerten, J.G.M., Geurts, B.J., 2014, Delay of biomass pyrolysis by gas-particle interaction. *Journal of Analytical Applied Pyrolysis*, 110, 88–99.
- Shampine, L. F., Reichelt, M. W., Kierzenka, J.A., 1999, Solving Index-1 DAEs in MATLAB and Simulink. *SIAM Review*, 41, 538–552.
- Stagni, A., Frassoldati, A., Cuoci, A., Faravelli, T., Ranzi, E., 2016, Skeletal mechanism reduction through species-targeted sensitivity analysis. *Combustion & Flame*, 163, 382–393.